A microfabricated ^{87}Rb vapor cell with dual-chamber for chip-scale atomic clock

Li Shaoliang[1,2], Xu Jing[1], Zhang Zhiqiang[1,2], Wu Yaming[1]

(1. State Key Laboratory of Transducer Technology, Shanghai Institute of Microsystem and Information Technology, Chinese Academy of Sciences, Shanghai 200050, China; 2. University of Chinese Academy of Sciences, Beijing 100049, China)

Abstract: Alkali vapor cell is one of the key components of chip-scale atomic clocks (CSACs), and its microfabrication is very significant yet challenging. Arrays of ^{87}Rb vapor cell with dual-chamber for CSACs were batch fabricated by MEMS technology. Pure ^{87}Rb vapor was produced by in-situ chemical reaction during anodic bonding process and buffer gas (N_2) was backfilled to ensure the pressure is precisely controlled. The dual-chamber structure helps to prevent the impurity after reaction from blocking light path, in order to improve the intensity of optical signal. Optical absorption spectrum of ^{87}Rb D1 line and the error signal used to lock the frequency of chip-scale atomic clock were finally obtained through experimental test. The peak-to-valley separation of the ^{87}Rb D1 line error signal can reach 0.53 kHz at 90 ℃, which indicates that the ^{87}Rb vapor cell can meet the requirement of CSACs or other chip-scale atomic devices (CSADs).

Key words: ^{87}Rb vapor cell; chip-scale atomic clock; coherent population trapping; dual-chamber structure; MEMS technology

CLC number: TN389 **Document code**: A **Article ID**: 1007-2276(2014)05-1463-06

一种微型化制造的双腔结构芯片原子钟 ^{87}Rb 蒸汽腔

李绍良[1,2],徐 静[1],张志强[1,2],吴亚明[1]

(1. 中国科学院上海微系统与信息技术研究所 传感技术联合国家重点实验室,上海 200050;
2. 中国科学院大学,北京 100049)

摘 要:碱金属蒸汽腔是芯片原子钟(CSACs)中重要的核心部件之一,其微型化制造具有重要的实用价值,同时也非常具有挑战性。采用 MEMS 技术批量化制作了具有双腔结构的芯片原子钟 ^{87}Rb 蒸汽腔阵列。在阳极键合过程中,通过原位化学反应产生纯净的 ^{87}Rb 元素蒸汽,缓冲气体(N_2)采用反充的方法充入到 ^{87}Rb 蒸汽腔内以保证缓冲气体的压强可以精确的控制。所设计的双腔结构可以防止原位化学反应中产生的杂质阻挡光路,从而能够提高探测到的光信号的强度。通过原子钟桌面系统测试,得到了 ^{87}Rb 元素 D1 线的光学吸收谱和用于芯片原子钟锁频的误差信号,在 90℃时,^{87}Rb 元素 D1 线

收稿日期:2013-09-17; **修订日期**:2013-10-17

基金项目:中科院院知识创新工程重要方向性项目(KGCX2-YW-143)

作者简介:李绍良(1987-),男,博士生,主要从事 MEMS 技术和微型 CPT 原子钟物理系统等方面的研究工作。
Email: lishaoliang@mailsim.ac.cn

导师简介:吴亚明(1966-),男,博士生导师,博士,主要从事光通信器件、光传感技术、光信号与光信息处理、微型 CPT 原子钟等方面的研究工作。Email:yamingwu@mail.sim.ac.cn

纠偏信号的线宽(波峰与波谷间距)可达到 0.53 kHz。测试结果表明,双腔结构的 ^{87}Rb 蒸汽腔满足芯片原子钟或其他芯片级原子器件的设计要求。

关键词: ^{87}Rb 蒸汽腔; 芯片原子钟; 相干布居数囚禁(CPT); 双腔结构; MEMS 技术

0 Introduction

Nowadays atomic clocks are the most accurate time and frequency standards, and play important roles in so many respects such as Global Position System (GPS) navigation and positioning, communication, time keeping and transport, some science fields and so on. However, the further wide application of atomic clocks is limited by their dimensions, price and power consumption. The miniaturization of atomic clocks is very meaningful yet challenging.

The Coherent Population Trapping (CPT) effect discovered in 1976, opens a way to the realization of chip-scale atomic clocks (CSACs). Figure 1 shows the basic working principle of CPT atomic clock. Two coherent laser beams, which are usually emitted from a local-oscillator-modulated semiconductor laser, pass through an alkali vapor cell which is a three-energy-level system. When the frequency difference of the two laser beams is equal to the frequency separation of the ground-state hyperfine splitting, the atoms are coherent coupled together and trapped into the ground state, a bright line of transmitted optical signal could be observed by a photodiode (PD). The signal detected by the PD could be processed by signal processing circuit to get error signal which is used to lock the frequency of atomic clock. Because there is no need of microwave cavity, it is easy to employ MEMS technology to realize the fabrication of CSACs. In 2002, Lutwak et al [1] described a laboratory CSAC based on CPT and made a comparison with conventional atomic clock . After that the realization of CSACs based on CPT effect has been widely studied in many countries [2-7].

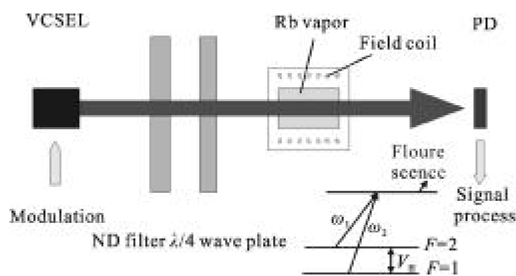

Fig. 1 Schematic diagram of the working principle of CPT-based atomic clock

So far there are many cell-filling techniques which have been explored for the microfabrication of MEMS vapor cell. At the very beginning, prototype vapor cells were manufactured via a hybrid process of MEMS cell fabrication combined with conventional glassblowing and direct alkali metal filling method [8]. Liew et al [9] for the first time realized the vapor cell by in-situ chemical reaction between cesium chloride (CsCl) and barium azide (BaN_6) during the bonding process, and more recently, they managed to produce Cs and buffer gas N2 by photolysis of cesium azide (CsN_3) after the bonding process [10]. Radhakrishnan et al [11] made use of enclosed alkali metals in a chemically inert wax to preform alkali metal-wax micro packets and the enclosed alkali metal was released into the cavity by laser ablating. Gong et al [5] proposed an electrolytic method to produce Cs after the cell was sealed.

Among these microfabrication methods of alkali vapor cell, the method of in-situ chemical reaction is one of the most adopted ways due to its lower requirement of operation environment, more simple process and easy-to-batch production. However the in-situ chemical reaction will generate impurities remained in the cavity which can block the light path and increase the Johnson noise of the signal [12]. Thereby the transmitted optical absorption spectrum quality is very poor and its related error signal accuracy may be reduced.

In this article, ^{87}Rb vapor cell with dual-chamber structure was fabricated by the method of in-situ chemical reaction, where the impurities were limited in one of the two chambers to avoid blocking the light path and the light passed through the other chamber. In the following sections, the dual-chamber structure of ^{87}Rb

vapor cell was first introduced, and then the MEMS fabrication process was illustrated in detail. By employing the in-situ chemical reaction method put forwards by Knappe et al[13] and controlling the anodic bonding process precisely, the vapor cell with dual-chamber for CSACs containing ^{87}Rb isotopes and buffer gas of N_2 was fabricated successfully. At last, the optical absorption spectrum of ^{87}Rb D1 line and the error signal used to lock the frequency output of CSACs were obtained through experimental test. The peak-to-valley separation of the error signal is about 0.53 kHz at 90 ℃. The experimental result indicates that the ^{87}Rb vapor cell with dual-chamber can meet the requirements of the CSACs and other chip-scale atomic devices[14].

1 Experimental procedure

1.1 Structure of the ^{87}Rb vapor cell with dual-chamber

Figure 2 shows the schematic structure of the 87Rb vapor cell. A "glass-silicon-glass" sandwich structure with dual-chamber is adopted. One chamber is reservoir for compound which is used to contain the compound as well as rubidium after the reaction. While the other chamber is optical window which only contains rubidium vapor and buffer gas. The two chambers were connected with a very shallow microchannel with the depth of less than 10 μm. The rubidium vapor can diffuse into the optical window from reservoir during the chemical reaction. The size of the vapor cell is 6 mm×4 mm×2 mm, and the size of optical window and reservoir are both 2 mm×2 mm, and the depth of the two chamber is 1.5 mm, which is determined by the thickness of silicon wafer.

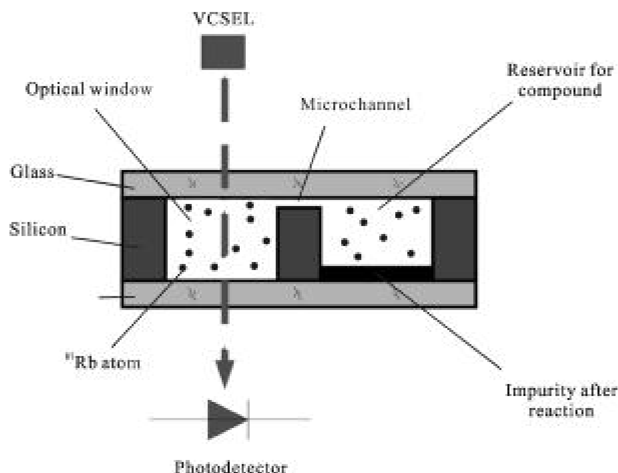

Fig.2 Structure of the ^{87}Rb vapor cell with dual-chamber

1.2 Fabrication procedure

The fabrication procedure is schematically shown in Fig.3. An N-type double-polished silicon wafer with <100> crystal direction was prepared and its thickness is 1.5 mm which is much thicker than ordinary silicon wafers in MEMS process. At first a shallow channel was fabricated by Deep RIE or wet etching as shown in Fig. 3(a). Then two films of Si_3N_4 and SiO_2 were deposited onto the silicon wafer successively by LPCVD technology(Fig. 3(b)). The etching window was patterned on both sides of the wafer by photolithography and wet etching of buffered oxide etching solution and hot phosphoric acid as shown in Fig. 3 (c). The wafer was then put into KOH etching solution for long time etching until the whole wafer was etching through to form the two chamber of vapor cell. The excellent corrosion resistance of Si_3N_4 in KOH solution made it endure the process very well. After that, a 250 μm thick Pyrex glass plate was anodically bonded to the silicon to produce a bonded preform as shown in Fig. 3(d). Then, we put the mixture of RbCl (^{87}Rb isotope) and BaN_6, which was made by dissolving them into water to form a clear colorless solution, into the reservoir with a transfer pipette, and then baked it in anaerobic environment until it changed back to white solid powder again (Fig. 3(e)). The solid powder was considered mixed very well for chemical reaction afterwards. The process of the chemical reaction can be summarized as following[15]:

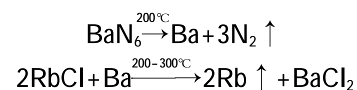

$$BaN_6 \xrightarrow{200℃} Ba + 3N_2\uparrow$$

$$2RbCl + Ba \xrightarrow{200-300℃} 2Rb\uparrow + BaCl_2$$

According to the chemical reaction equation, the mass ratio of RbCl to BaN_6 is 1:0.915. Due to the possibility that the barium residue remained in the cell after the chemical reaction could recombine with the buffer gas (N_2) again, thus result in decreasing the N_2 pressure over time and causing a drift in the CPT frequency[13], the mass of RbCl was chosen slightly surplus.

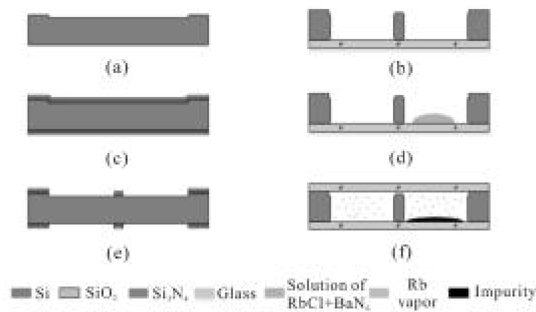

Fig. 3 Fabrication process of 87Rb vapor cell

Finally, the bonded pre-form with compound inside was placed on clamp of the bonder, and a 250 μm thick Pyrex glass was placed above it, and three 100 μm thick spacers of the clamp were placed between the two wafers to make sure there was a gap between them. Then the clamp carrying the wafers was pushed into vacuum chamber of anodic bonder and the pressure could be pumped to 3.0×10^{-6} mBar. Then the hot plate was heated slowly to 200 ℃ and kept for hours which is long enough to make sure that BaN_6 was decomposed into Ba and N_2 completely. The N_2 generated was pumped out and then buffer gas was backfilled in order to control the type and pressure of buffer gas precisely. Here the adopted buffer gas is N_2 and the range of the pressure could be 10 mBar to 300 mBar. After that the spacers were taken out and hot plate was heated to 300 ℃, and a 1 200 N force, 800 V voltage were applied upon the wafers to complete anodic bonding. Subsequently, the whole wafer could be kept at 300 ℃ for 30 min or more to guarantee that the compound was reacted completely. At last, the bonded wafer should be diced into individual cells and a chip of microfabricated 87Rb vapor cell with dual-chamber was obtained as shown in Fig. 3(f).

2 Experimental results

2.1 Observation of the ^{87}Rb metal in the Cell

Figure 4 (a) shows the wafer of the ^{87}Rb vapor cell before dicing. Figure 4 (b) is the partial enlarged view of ^{87}Rb vapor cell. In one cell, the upside is the reservoir window and the downside is the optical window. The black solid materials in the reservoir are the impurity after chemical reaction composed of $BaCl_2$ and a small quantity of unreacted RbCl, which make it almost optically non-transparent. The shiny spots on the inside surface of upper Pyrex glass are the metal ^{87}Rb, which make it clear that the produced ^{87}Rb vapor has diffused into optical window from the reservoir and condensed on the inside surface of the glass.

The whole wafer is uniform and good in both aspect of producing Rb and bonding effect. As shown in Fig.4 (b), due to the amount of solution dropped into the reservoir is different between rows, the amount of Rb produced is different. For an appropriate amount of solution dropped, the ratio of the cell producing Rb in the whole wafer is more than 99%. As shown in Fig.4 (a), the bonding effect of whole wafer is uniform overall except for a small unbonded area which may be caused by particles on the bonding surface. The ratio of the area bonded successfully in the whole wafer is more than 96%.

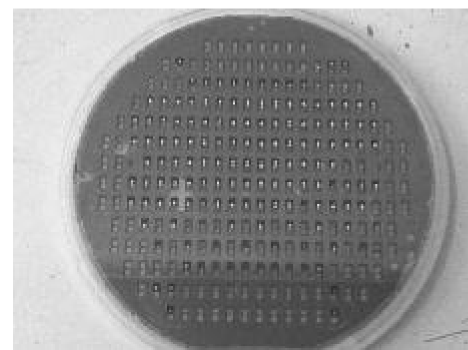

(a) Wafer of ^{87}Rb vapor cell

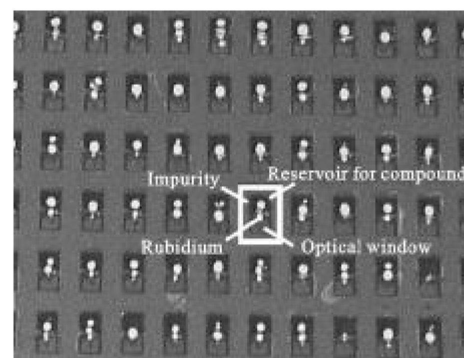

(b) Partial enlarged view of the wafer

Fig.4 Photograph of ^{87}Rb vapor cells

2.2 Optical absorption spectrum

The existence of ^{87}Rb in the cell was confirmed by the test of optical absorption spectrum. Figure 5 shows the experimental setup for measuring the optical absorption resonance. By modulating the sweeping current of current source, the wavelength of the VCSEL was scanned over near 795 nm. When the laser beam passed through the vapor cell, which was heated to a controlled temperature ranging from room temperature to 120 ℃, the transmitted light power was tested by a photodiode (PD) and shown on an oscilloscope at the same time. Experiment test show that when the ^{87}Rb vapor cell was heated to above 75 ℃, the optical absorption spectrum could be observed obviously. Figure 6 shows the two peaks separated by the ground-state hyperfine splitting of ^{87}Rb (6.8 GHz) when the cell was heated to 100 ℃.

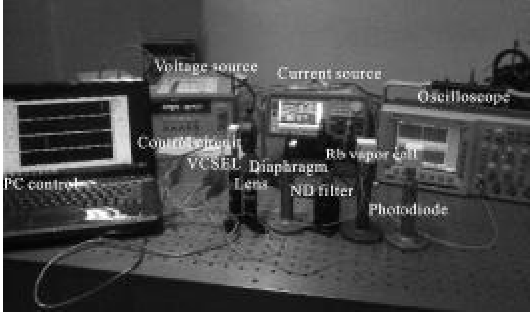

Fig. 5 Experimental setup for measuring optical absorption spectrum

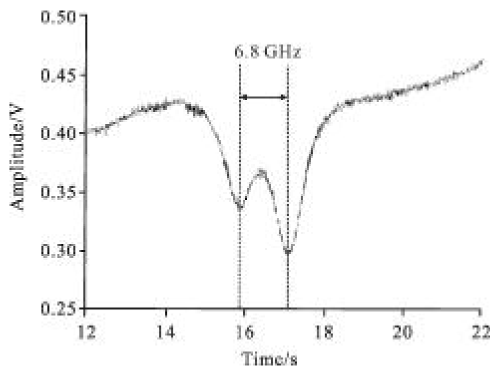

Fig.6 Optical absorption spectrum of ^{87}Rb vapor cell at 100 ℃

2.3 Error signal

The error signal of ^{87}Rb D1 line obtained from a microfabricated ^{87}Rb vapor cell was obtained in the experiment. The current of VCSEL was modulated at 3.4 GHz (one-half of the ground-state splitting of ^{87}Rb). The diameter of VCSEL beam is about 2 mm and its light intensity is 25 μW which is measured in front of ^{87}Rb vapor cell. The temperature of ^{87}Rb vapor cell was precisely controlled at 90 ℃. The photodiode behind the ^{87}Rb vapor cell could detect the optical absorption spectrum. Afterwards the spectrum detected by PD was processed by phase-sensitive demodulation circuit to obtain error signal which was used to lock the frequency of atomic clock. Figure 7 shows the error signal of ^{87}Rb D1 line under the condition described above. The peak-to-valley separation of the error signal can reach 0.53 kHz at 90 ℃ and theoretically the Full Width at Half Maximum (FWHM) of the CPT signal of ^{87}Rb D1 line is about 0.918 kHz. It indicates that the ^{87}Rb vapor cell with dual-chamber can meet the experimental requirements of CSACs.

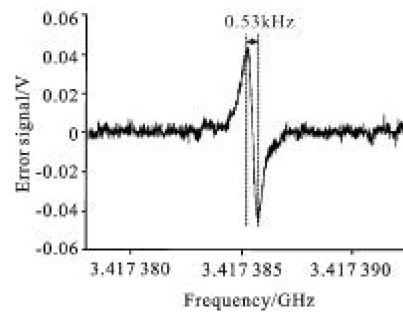

Fig.7 Error signal of the ^{87}Rb vapor cell at 90 ℃

3 Conclusion

In this article, we realized the microfabrication of ^{87}Rb vapor cell with dual-chamber for chip-scale atomic clock based on MEMS technology. The ^{87}Rb vapor cell was adopted dual-chamber structure during the MEMS process in order to make the optical path more optical transparent by avoiding the impurity after chemical reaction blocking the optical path, and increase the intensity of optical absorption spectrum of ^{87}Rb D1 line. The pure ^{87}Rb vapor was produced by in-situ chemical reaction of barium azide (BaN_6) and rubidium chloride (RbCl). The buffer gas was backfilled during the anodic bonding process which can make sure to control the type and pressure of buffer gas precisely, and the type of buffer

gas here we adopt is N_2 for now. The transmitted optical signal of ^{87}Rb D1 line and the error signal which is used to lock the frequency of chip -scale atomic clock were finally obtained through the experimental test. The peak-to-valley separation of the error signal can reach to 0.53 kHz at 90 ℃, and theoretically the FWHM of the CPT signal of ^{87}Rb D1 line is about 0.918 kHz which can meet the requirements of the CSACs. The next work we will do is trying to backfill proper type of buffer gas mixture with complementary frequency drift coefficient and test the frequency stability of the CSACs packaged into servo circuit system.

References:

[1] Lutwak R, Emmons D, Riley W, et al. The chip-scale atomic clock - coherent population trapping vs conventional interrogation [C]//34th Annual Precise Time and Time Interval (PTTI) Meeting, 2002.

[2] Kitching J, Knappe S, Hollberg L, et al. Miniature vapor-cell atomic-frequency references [J]. Applied Physics Letters, 2002, 81(3): 553-555.

[3] Knappe S, Vishal S, Schwindt P, et al. A microfabricated atomic clock [J]. Applied Physics Letters, 2004, 85(9): 1460-1462.

[4] Zhu M, Cutler L, Berberian J E, et al. Narrow linewidth CPT signal in small vapor cells for chip scale atomic clocks [C]//2004 IEEE International Frequency Control Symposium and Exposition, 2004.

[5] Gong F, Jau Y Y, Jensen K, et al. Electrolytic fabrication of atomic clock cells [J]. Review of Scientific Instruments, 2006, 77: 076101-3.

[6] Goka S. Rb-85 D1-line coherent-population-trapping atomic clock for low-power operation [J]. Japanese Journal of Applied Physics, 2010, 21::1508-1513.

[7] Knapkiewicz P, Dziuban J, Walczak R, et al. MEMS caesium vapour cell for European micro-atomic-clock [J]. Procedia Engineering, 2010, 5:721-724.

[8] Lutwak R, Emmons D, English T, et al. The chip-scale atomic clock - recent development progress [C]// 35th Annual Precise Time and Time Interval (PTTI) Meeting, 2003.

[9] Liew L, Knappe S, Moreland J, et al. Microfabricated alkali atom vapor cells [J]. Applied Physics Letters, 2004, 84 (14): 2694-2696.

[10] Liew L, Moreland J, Gerginov V. Wafer-level filling of microfabricated atomic vapor cells based on thin-film deposition and photolysis of cesium azide [J]. Applied Physics Letters, 2007, 90(11): 1141061-3.

[11] Radhakrishnan S, Lal A. Alkali metal-wax micropackets for chip-scale atomic clocks [C]//The 13th International Conference on Solid-state Sensors, Actuators and Microsystems, 2005.

[12] Griffith W C, Knappe S, Kitching J. Femtotesla atomic magnetometry in a microfabricated vapor cell [J]. Optical Express, 2010, 18(26): 27167-27172.

[13] Knappe S, Schwindt P, Shah V, et al. A chip-scale atomic clock based on ^{87}Rb with improved frequency stability [J]. Optical Express, 2005, 13(4): 1249-1253.

[14] Kitching J, Knappe S, Donley E A. Atomic sensors - a review [J]. IEEE Sens J, 2011, 11(9): 1749-1758.

[15] Su J, Deng K, Guo D Z, et al. Stable Rb-85 micro vapour cells: fabrication based on anodic bonding and application in chip-scale atomic clocks [J]. Chinese Physics B, 2010, 19 (11): 1107011-8.